

Light torque nanocontrol, nanomotors and nanorockers

Keith D. Bonin and Bakhit Kourmanov

Department of Physics, Wake Forest University, Winston-Salem, NC 27109, USA
bonin@wfu.edu

Thad G. Walker

Department of Physics, University of Wisconsin, Madison, WI 53706 USA

Abstract: In a novel application of light torques, we manipulate and control the rotation of nanorods. We apply light torques to 250 nm diameter glass nanorods in a single-beam optical trap. Light-torque operated nanomotors whirl at moderate speeds that depend on several factors, including the magnitude of the light torque, the viscosity of the surrounding medium, and the rotation rate of the electric field vector of the linearly polarized trapping light. Two new modes of behavior - rocking motion and saltatory motion - are also described and explained.

©2002 Optical Society of America

OCIS codes: (140.7010) Trapping, (350.0350) Other areas of optics, (350.4990) Particles

References and links

1. A. Ashkin, "Optical trapping and manipulation of neutral particles using lasers," Proc. Nat. Acad. Sci. **94**, 4853 (1997).
2. L. Paterson, M.P. MacDonald, J. Arlt, W. Sibbett, P.E. Bryant, and K. Dholakia, "Controlled rotation of optically trapped microscopic particles," Science **292**, 912 (2001).
3. M.P. MacDonald, L. Paterson, K. Volke-Sepulveda, J. Arlt, W. Sibbett, and K. Dholakia, "Creation and manipulation of three-dimensional optically trapped structures," Science **296**, 1101 (2002).
4. R.C. Gauthier, M. Ashman, and C.P. Grover, "Controlled rotation of optically trapped microscopic particles," Appl. Opt. **38**, 4861 (1999).
5. A.T. O'Neil, M.J. Padgett, "Rotational control within optical tweezers by use of a rotating aperture," Opt. Lett. **27**, 743-745 (2002).
6. M.E.J. Friese, T.A. Nieminen, N.R. Heckenberg, and H. Rubinsztein-Dunlop, "Optical alignment and spinning of laser-trapped microscopic particles," Nature **394**, 348 (1998).
7. E. Higurashi, H. Ukita, H. Tanaka, and O. Ohguchi, "Optically induced rotation of anisotropic micro-objects fabricated by surface micromachining," Appl. Phys. Lett. **64**, 2209 (1994).
8. T.B. Jones, *Electromechanics of Particles*, (Cambridge University Press, New York, 1995).
9. Z.-P. Luo, Y.-L. Sun, and K.-N. An, "An optical spin micromotor," Appl. Phys. Lett. **76**, 1779 (2000).
10. P. Galadja and P. Ormos, "Complex micromachines produced and driven by light," Appl. Phys. Lett. **78**, 249 (2001).
11. A. Ashkin and J.M. Dziedzic, "Optical trapping and manipulation of viruses and bacteria," Science **235**, 1517 (1987).
12. K. Svoboda and S. Block, "Optical trapping of metallic Rayleigh particles," Opt. Lett. **19**, 930 (1994).
13. M.M. Tirado and J.G. de la Torre, "Rotational dynamics of rigid, symmetric top macromolecules. Application to circular cylinders," J. Chem. Phys. **73**, 1986 (1980).
14. E. M. Purcell, "Life at low Reynolds number," Am. J. Phys. **45**, 3 (1977).
15. T.R. Strick, V. Croquette, and D. Bensimon, "Single-molecule analysis of DNA uncoiling by a type II topoisomerase," Nature **404**, 901 (2000).
16. R.K. Soong, G.D. Bachand, H.P. Neves, A.G. Olkhovets, H.G. Craighead, and C.D. Montemagno, "Powering an inorganic nanodevice with a biomolecular motor," Science **290**, 1555 (2000).
17. K. Kinoshita, R. Yasuda, H. Noji, and K. Adachi, "A rotary molecular motor that can work at near 100% efficiency," Phil. Trans. R. Soc. Lond. B **355**, 473 (2000).

Application of controlled light *forces* to microscopic and nanoscopic particles is a major success of modern optics [1]. A remaining challenge is to apply controlled light *torques* to *nanoscale* particles at a similar level of control. Previous techniques for applying light

torques have all been used on microscopic particles and suffer from optical complexity [2,3], a lack of independent translational and orientational control [2-5], an inability to extend to the nanoscale [2-5], or were only applied to birefringent crystals [6]. Here we show how to apply controlled torques to asymmetric nanoparticles using a simple and broadly accessible light-polarization optical trap. We thereby operate light torque nanomotors that rotate at moderate speeds. Previous light torque techniques produced micron-sized motors [3-10]. Optical vortices, which are useful for creating micrometer scale micromachines [2,5,6], have been recently used to create three-dimensional trapped structures [3]. We also operate light torque nanorockers, generating a novel class of nanoscale motion whereby nanorods oscillate between two fixed angles. In addition, we have generated another novel class of motion - saltatory rotation, where the rotation rate varies with angle in a reproducible way. We control our rotation and rocking frequencies without changing the magnitude of the trapping force, and our modest laser powers should allow interesting biological applications. A simple model explains observed behavior and directly applies to smaller systems.

A simple optical tweezers setup of very modest laser power (20 mW) trapped cylindrical borosilicate glass fibers of average diameter $d = 260$ nm and lengths of 2-5 μ m. The light trap was made using a 100x, NA=1.3 oil-immersed objective. The nanorods were held transversely in the optical trap, just above the surface of the microscope slide, by laser light at wavelength $\lambda = 514$ nm. The laser's trapping waist was about 0.5 μ m. Light polarization was controlled by adjusting the angle of a half-wave plate relative to the light's original polarization axis. The half-wave plate rotates the polarization direction of transmitted light by twice the angle of rotation. We measured the light to be linearly polarized at the entrance to the objective to better than one part in 3000.

All previous light-driven motor experiments [3-10], which produced micron-sized motors, can be understood with ray optics. In contrast, here the important particle dimension d is half the wavelength of light, and we operate in the regime between Rayleigh ($d \ll \lambda$) and ray optics ($d \gg \lambda$). Since $d < \lambda$ and since we plan to investigate even smaller spatial regimes, we discuss the basic light-particle interaction in the Rayleigh limit. We assume the trapped particle is a homogeneous, asymmetric, nonabsorbing dielectric object immersed in a dielectric liquid. The linearly polarized electric field of the laser beam \mathbf{E} induces a dipole moment $\mathbf{p} = \tilde{\alpha} \mathbf{E}$, where $\tilde{\alpha}$ is the polarizability tensor of the nanoparticle. It is energetically favorable for the induced dipole moment \mathbf{p} and, hence, the particle to rotate to align with the field - see Fig. 1. The resulting torque, $\boldsymbol{\tau} = \mathbf{p} \times \mathbf{E}$, is proportional to the polarizability difference $\alpha = \alpha_{\parallel} - \alpha_{\perp}$. That such a torquing interaction occurs at the nanoscale was first suggested by Ashkin [11] as a result of the change in observed pattern of scattered light from the tobacco mosaic virus. In the ray-optic limit, applicable to much larger microrods, it was theoretically predicted and experimentally confirmed that microrods with flat endfaces can display a modest tilt of their long axis with respect to the laser propagation axis [4]. For the nanorods described here, where ray-optics analysis does not apply, such a tilt was not observed. Note that, like the case of optical trapping of spheres, Brownian motion is not a problem at any size scale as long as suitable trapping power is applied. However, a potential limitation to the size scale of *single-beam* optical tweezing, and to the single-beam light torque described here, is absorption [12]. Particles as small as 20-40 nm diameter have been optically trapped with a single beam [12].

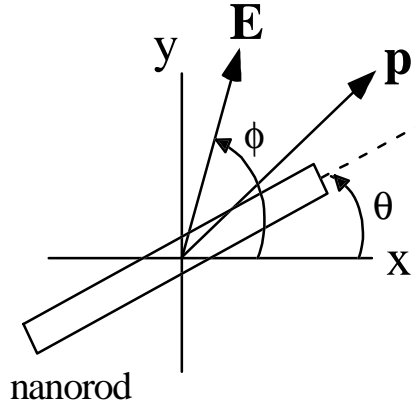


Fig. 1. A sketch of the light torque geometry. Here the induced dipole \mathbf{p} will move to align with the electric field \mathbf{E} to minimize energy. Hence, a torque $\boldsymbol{\tau} = \mathbf{p} \times \mathbf{E}$ exists about an axis out of the plane of the paper.

The nanomotor and nanorocker behaviors can be understood using a model based on Newton's second law. In addition to the light torque, the rotating particle experiences a damping torque due to the surrounding medium. The resulting equation of motion is, with $\dot{\phi} = \Omega t$ (see Fig.1),

$$I\ddot{\theta} = U \sin[2(\Omega t - \theta)] - \gamma\dot{\theta} \quad (1)$$

where the dot over a function indicates a time derivative; I is the moment of inertia of the nanoparticle; $U = -\alpha E_0^2/4$ is the trapping potential (time-averaged over one optical cycle); θ is the angle of the nanorod axis with respect to a fixed laboratory frame axis; Ω is the angular rotation frequency of the light polarization axis; and γ is the angular drag coefficient from Stokes law for rotation in a viscous medium [13]. Under steady state rotation, the electric field leads the induced dipole direction by $\beta = (1/2)\sin^{-1}(\gamma\Omega/U)$, i.e. $(\Omega t - \theta) = \beta$. The inertial term on the left side of Eq.(1) can be ignored under nanomotor circumstances, since inertial forces and torques are much smaller than drag forces and torques at low Reynolds number [14]. For example, under typical nanomotor conditions $I\ddot{\theta}/\gamma\dot{\theta} \approx 10^{-7}-10^{-8}$. Ignoring the $I\ddot{\theta}$ term in Eq.(1) gives

$$\dot{\theta} = \frac{U}{\gamma} \sin[2(\Omega t - \theta)]. \quad (2)$$

The steady-state solution to Eq.(2) is $\sin(2\beta) = \gamma\Omega/U$. Thus when $\gamma\Omega/U < 1$, the motion is that of a continuous nanomotor in phase with the polarization rotation. However, when $\gamma\Omega/U > 1$, phased motion is not allowed and the rotation becomes interrupted. Microscopes can produce a slight intensity ellipticity at the waist of a Gaussian beam – the resulting torque is negligible (< 1% of the polarized light torque).

Subject to static and rotatory torques, we observe three distinct behaviors of the glass nanorods: discrete steps, rotational motion, and rocking. We confirmed the polarized-light torque by observing discrete motion of the trapped rods when the laser polarization was rotated by manually rotating the polarization optic - see Fig. 2(a). The polarization is in the plane of each image, and the nanorods align along the direction of polarization.

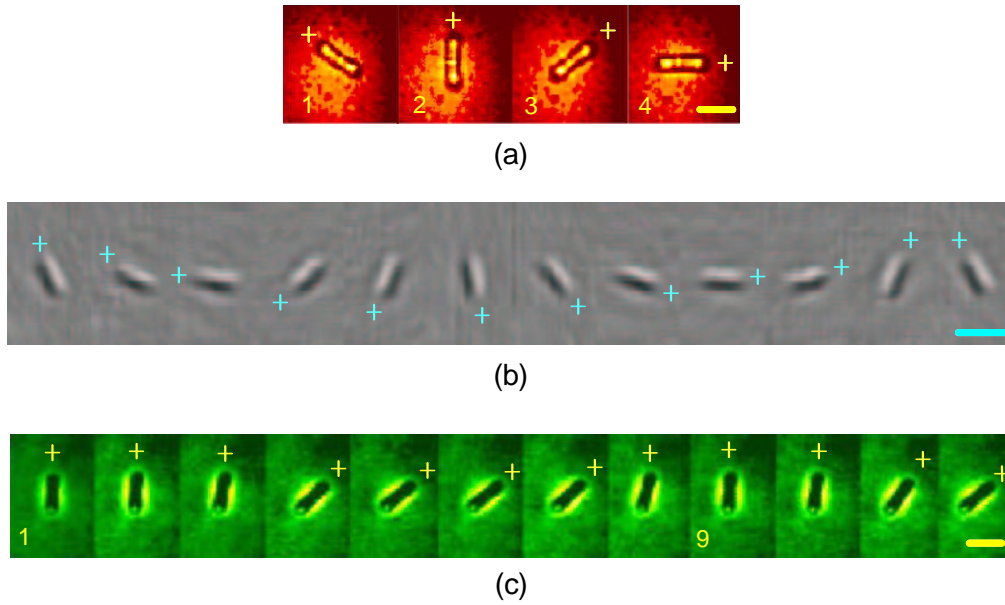


Fig. 2. Image sequences showing the three different types of motion. In each frame a + symbol labels the orientation of the rod and the scale bar is $3 \mu\text{m}$. (a) Discrete nanorod manipulation: the light polarization is discretely oriented by a manual rotation of the polarization optic at the following angles with respect to a horizontal line: (1) 45, (2) 90, (3) 135, (4) 180. (b) Nanomotor behavior: the rod rotates in response to a rotating polarization light torque. (c) Nanorocker behavior: here the rod rocks in response to a rotating polarization light torque. In frame # 9, the nanorod has completed one full period of rocking.

A light-torque nanomotor was achieved by continuously rotating the laser polarization with the half-wave plate - see Fig.2(b). Two critical observations confirm that we are observing a light-torque effect and not an intensity gradient effect due to some potential beam movement as the $\lambda/2$ plate is rotated:

- (1) As in the static case, when the half-wave plate is rotated by angle θ , the rods rotate twice the angle.
- (2) The nanomotors clearly rotate about their midpoint, and if trapped at one end, a rod will not rotate.

To understand the last point, note that the viscous drag γ on a cylindrical rod rotating about its midpoint depends on its length L according to [13]

$$\gamma \approx \frac{\pi\eta L^3}{3[\ln(L/2a) - 0.66]} \quad (3)$$

Here, η is the viscosity of the medium, and a is the rod radius. Therefore, a rod trapped at its midpoint experiences a much-reduced drag compared to a rod trapped at one end. Also, rods trapped at the center cannot be rotated by physically moving the trap focal spot around in a circle.

When varying conditions, like the polarization rotation rate and/or the trap location along the rod, rocking motion was also observed --- see Fig. 2(c). Here, the nanorod rotated over a finite angular range $\Delta\theta$, stopped for some time, and then rotated back to its original position. For example, the rod pictured in Fig.2(c) was 'rocked', for a 10-minute interval, over a range of frequencies that varied by a factor of 40 ($0.4 \text{ Hz} \leq \Omega/2\pi \leq 16 \text{ Hz}$). The angular range, $\Delta\theta$, decreased with increasing rotation frequency - see Fig. 3. Figure 3 (inset) is a plot of the angle as a function of time for the nanorocker shown in Fig. 2(c). In all cases, the rocking

frequency matched the polarization rotation frequency to within experimental error. In some cases, a rod rocking at a frequency below 1 Hz changed over into a nanomotor with no obvious change in external conditions.

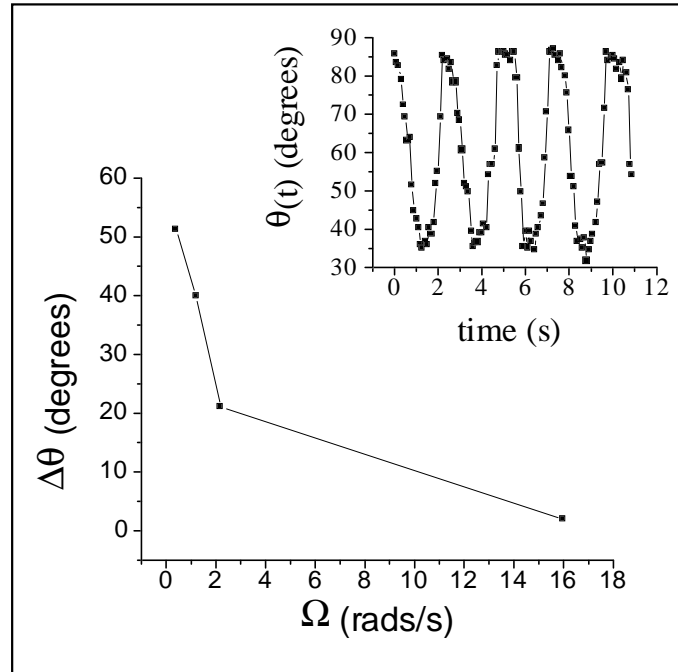


Fig. 3. A plot of the angular range $\Delta\theta$ versus laser polarization rotation frequency Ω for a single nanorod undergoing rocking motion. **Inset:** A plot of the angle versus time for the glass nanorod in Fig. 2(c) - operated in nanorocker mode.

Several features of the nanomotor motion agree with the theoretical model. First, the direction of rod rotation depended on the direction of rotation of the electric field polarization. Second, the rotation rate of the nanomotor matched the rotation rate of the laser polarization over the observed range of $0.1 \text{ Hz} \leq \Omega / 2\pi \leq 1 \text{ Hz}$. No nanomotor ever exceeded a maximum rotation frequency of 1 Hz, which is probably determined by a combination of rod size and trapping power. At higher frequencies the nanomotor would lock at an angle (if it was a nanorocker) or it would appear to move randomly. At low frequencies, the motion was chaotic, with momentary direction reversals and frequent translations along the rod symmetry axis. The translations are easily explained by noting that both the trapping force and the light torque are invariant under such translations. Finally, an online movie (see Fig. 4) clearly shows that the nanomotor experiences periods of interruption, where the angle is momentarily stationary. Such saltatory behavior is readily obtained from solutions to Eq.(2) when $\gamma\Omega/U > 1$.



Fig. 4. (1.28 Mb) Polarized-light torque nanomotor: a glass rod in an optical trap rotating due to the torque applied by rotating the polarization of the trapping light. Note the interrupted, or saltatory, motion of the nanorod. The glass rod is $2.5 \mu\text{m}$ long and 260 nm in diameter.

To explain the nanorocker motion, consider the case where the polarization rotation rate exceeds the rotation rate of the nanorod due to viscous drag. Then, the electric field vector eventually aligns itself with the induced dipole moment, which momentarily results in zero applied light torque before the light torque reverses direction. Here, the equation of motion is significantly changed so that the inertial term, previously ignored, becomes important. The angular velocity becomes overdamped in $\gamma/I = 100$ ns. This damping brings the rod to a rest, at which point interaction with the surface can become more significant than it was during motion. As the polarization vector continues its rotation, the light torque grows again (but reversed in direction) until the torque exceeds the threshold needed to get the nanorod moving again. The cycle then repeats itself in the opposite direction. The critical feature required to model rocking motion is the existence of a threshold torque for overcoming the increased interaction with the surface when at rest. To model such behavior, the equation of motion was modified by multiplying the rotational velocity $\dot{\theta}$ by a step function that forced the velocity to be zero once the velocity dropped below a certain preset value. An additional subtle factor that can cause a transition from rocking to motor behavior (or vice versa) at a given polarization rotation frequency is translation of the rod along the symmetry axis. Rockers tend to occur when the trapping point is offset from the midpoint, while motors rarely occur with the trap off the midpoint. An additional supporting observation is that the motor would rapidly move through the 'allowed' finite angular rocking range, and would rotate more slowly through angular regions the rocker did not reach – such periodically slowed motion is labeled saltatory in biological systems. Hence, the nanorocker to nanomotor transition at frequencies below 1 Hz depends on a subtle interplay between rod translation during rotation and an increase in viscous drag when the trap is off center.

To conclude, we have shown that the polarized-light torque has many important advantages: it is simple, quite general, works for both nonabsorbing and absorbing particles, obeys a simple physical model, and can be readily extended to size regimes below the optical resolution limit. We can manipulate and orient asymmetric nanoparticles at discrete angles and easily coax them into behaving as nanorockers. Our technique has the potential to measure optical properties of single nanoparticles and to control and manipulate nanotubes and nanowires, important elements in nanoelectronics. The method can also be applied to measure the viscosity of nanoenvironments, a goal in many biological and rheological systems. Studies involving torques or torsion, such as the torsional analysis experiments of biomolecules like DNA [15], are strong candidates for our technique. Finally, polarized-light torques could also help clarify the behavior of rotational biomotors. For example, recent investigations of rotating nickel nanorods [16] and microtubules [17] attached to the shafts of F_0, F_1 -ATPase biomolecular motors have helped elucidate the fundamental behavior of these important biomechanical systems. The light torque could be used to study these molecular motors under varying conditions, such as ATP concentration and torsional load. In fact, the nickel nanorods used to observe the rotary motion in ATPase molecular motors were 750 nm long and 150 nm in diameter - only slightly smaller than the light-torqued glass nanorods used here.

Acknowledgements: We thank the Johns-Manville Corporation for providing glass fibers. B. K. thanks Wake Forest University for their support; T.G.W. was partially supported by the NSF. We also thank Robert Morris and Jeremy Qualls for technical assistance; George Holzwarth, Jeff Weiner, and Robert Swofford for the loan of critical equipment; and Martin Guthold and Mark Eriksson for careful readings of the manuscript.